Changes in boundary layer height drive the dry–wet changes during 1900-2010 in East Asia drylands

wenqian mao
Lanzhou University
yanru zhao
Fudan 7 University
yanling guo (mdycmwq@163.com)
Lanzhou University
wenyu zhang
Lanzhou University
wennan leng
Lanzhou University

Research Article

Keywords: Boundary layer, Dry–Wet climate, East Asia drylands, Change, 110 years

Posted Date: May 4th, 2021

DOI: https://doi.org/10.21203/rs.3.rs-471287/v1

Changes in boundary layer height drive the dry–wet changes during 1900-2010 in East Asia drylands

Wenqian Mao[1], Yanru Zhao[3], Yanling Guo[1], Wennan Leng[1,4], Wenyu Zhang[1,2]

1. Key Laboratory for Semi-Arid Climate Change of the Ministry of Education, College of Atmospheric Sciences, Lanzhou University, Lanzhou, 730000, China
2. School of Geoscience and Technology, Zhengzhou University, Zhengzhou, 450001, China
3. Department of atmospheric and Oceanic Sciences Institute of atmospheric sciences, Fudan University, Shanghai, 200000, China
4. Gansu Weather Modification Office, Lanzhou, 730000, China

Correspondence to: Yanling Guo（guoyl17@lzu.edu.cn）

Abstract. Based on data obtained from ERA-20C during 1900-2010, this study statistically conducted spatial-temporal characteristic and interrelation of boundary layer height (BLH) and aridity index (AI) in East Asia drylands, thus originally understanding dry-wet changes from perspective of atmospheric boundary layer. The results show high (low) BLH values generally coincide with regions that have small (large) AI values with a negative correlation for annual variability, and correlation coefficients were -0.469、-0.880、-0.947; and of which 61.3%、55.9%、55.9% of the years followed corresponding correlation, and 12.6%、8.1%、9.9% of the years reflected changes in BLH advanced AI changes for hyper-arid, arid, and semiarid regions, respectively; in addition, BLH and area of East Asia drylands exhibited a positive correlation coefficient of 0.651. These results indicate that there is a connection between BLH changes and dry-wet changes, confirming the phenomenon that changes in BLH drive dry-wet changes.

Keywords: Boundary layer; Dry–Wet climate; East Asia drylands; Change; 110 years;

Highlights:

1、Statistical and comparative analyses were conducted using reanalysis data spanning more than 100 years.

2、Boundary layer height has a negative correlation with aridity index for annual variability in different subtypes.

3、The degree of influence of changes in the BLH on the dry–wet climate changes was quantitatively calculated.

Declarations

1. Funding

This work was jointly supported by the National Natural Science Foundation of China under grant (41875085、41630421、41741023) from Wenyu ZHANG.

2. Conflicts of interest/Competing interests

Nothing.

3. Availability of data and material

Data of this work is from the European Centre for Medium-Range Weather Forecast

4. Code availability

This work mainly uses GrADS.

5. Authors' contributions

Wenqian Mao: Conceptualization, Writing-Original draft preparation Methodology.

Yanru Zhao: Investigation, Visualization.

Yanling Guo: Conceptualization, Writing- Reviewing and Editing.

Wennan Leng: Data curation, Software.

Wenyu Zhang: Supervision, guidance.

6. Ethics approval (include appropriate approvals or waivers)

Approvals.

7. Consent to participate (include appropriate statements)

All the authors participate this process.

8. Consent for publication (include appropriate statements)

We agree to publish in this journal

1 Introduction

Drought, one of the most major natural disasters, can cause economic losses amounted up to hundreds of billions of dollars every year (Brewer et al, 2011). Drylands, accounting for approximately 41% of global terrestrial land surfaces, make them as some of the most sensitive areas to climate change because of sparse vegetation coverage、high reflectivity、less precipitation and high evaporation (White and Nackoney, 2003; Ji et al., 2015). Under the long-term global warming, development of aridification shows a trend of strengthening, as well occurrence of extreme drought events increasing (Dai，2013; Zhang et al, 2015). Thus, dry-wet changes, especially on the drylands, have a significant impact on human activities and social sustainable development (Huang et al., 2017).

Previous studies about dry-wet changes mainly focus on some aspects such as global warming、sea surface temperature anomalies and atmospheric circulation changes (Trenberth et al., 2014; Huang et al., 2017). While, atmospheric boundary layer (ABL) as the important medium for material and energy exchange between the Earth's surface and the free atmosphere (Schmid et al, 2012; Compton et al, 2013), plays a critical role in atmospheric regulation at the weather and climate scales (McGrath-Spangler, 2016). And changes in the BLH over drylands are also actually related to the dry-wet changes. For example, BLH is higher in dry period than in wet period (Reddy et al., 2002); and ultrahigh boundary layers often occur in extreme arid desert areas (Takemi, 1999; Marsham et al., 2008); along with there is a negative correlation between daily maximum BLH and number of precipitation days in the same year (You et al., 2010; Wang et al., 2016). In this way, it is worthwhile to understand dry-wet climate change from the perspective of ABL, which can provide more abundant information for perceiving and comprehending climate change.

On the other hand, in terms of raindrop loss, it is found that the falling distance of raindrops has an opposite relationship with precipitation. Consequently, when there is the deeper boundary layer it obtains a greater raindrops evaporation rate and after the smaller precipitation, which contribute to the more severe the aridification (Rosenfeld et al., 1988; Itano, 1997; 1998). Maximum Mixed Layer thickness makes a difference on the northwest arid climate, lying in the thicker Mixed Layer and less precipitation cause the drier climate (Li et al., 2009; 2012). These studies preliminarily reveal the influence of boundary layer height on dry-wet variation.

BLH is an important parameter that is often used to represent the ABL's moisture holding capacity, determining the boundary layer property to the speed of response to external forcing (Ahlgrimm et al., 2006). Easu et al. (2008; 2010) found that changes in BLH had an impact on temperature changes by altering the effective heat capacity of atmosphere (Davy et al., 2016). Following the similar thought and combined with the preceding analysis, when the local BLH changes it can lead to the changes in air environmental capacity and bring about ABL's vapor column concentration changes, which further affect precipitation, evaporation, etc. and finally influence dry-wet change. However, can changes in BLH have an impact that through its influence on atmospheric water vapor and then affects dry-wet changes?

East Asia drylands cover most of East Asia zones, including northern China、Mongolian Plateau and parts of Central Asia. And they are home to 90% people live in developing countries where the associated population density is higher than that in other arid regions (Huang et al., 2017). In this study, ERA-20C reanalysis data during 1900-2010 were used to analyze BLH changes and AI changes in East Asian dryland, and the authenticity and accuracy of above ratiocination were originally considered.

2、Materials and methods

2.1 Data on BLH and AI

ERA-20C was the first atmospheric reanalysis dataset designed specifically for climate applications from the European Center for Medium-Range Weather Forecasts (Poli et al., 2016). The reanalysis dataset is based on the assimilation of surface observations obtained continuously over one century. In this study, monthly BLH, precipitation, land surface air temperature, and other related physical quantities recorded during 1900-2010 at a spatial resolution of 0.25° × 0.25° were obtained from the ERA-20C, which provides the conditions for analyzing the climatic characteristics of long time series. Two main methods were used to calculate the BLH in ERA-20C (ECMWF, 2014): an entraining parcel method used under convective conditions, and a bulk Richardson method used under neutral and stable conditions.

The AI is defined as the ratio of annual precipitation (P) to annual potential evapotranspiration (PET) (Huang et al., 2017),which reflects the scarcity of water supply relate to moisture demand of atmospheric.

The Penman–Monteith algorithm recommended by the Food and Agriculture Organization (FAO: http://www.fao.org/) was used to estimate PET in this study.

$$\mathrm{PET} = \frac{0.408\Delta(R_n - G) + \gamma \frac{900}{T_a + 273} u_2 (e_s - e_a)}{\Delta + \gamma(1 + 0.34u_2)}, \quad (1)$$

where Rn is net radiation at the surface ($MJ \cdot m^{-2} \cdot d^{-1}$), G is the soil heat flux density ($MJ \cdot m^{-2} \cdot d^{-1}$), es and ea are the saturation and actual vapor pressure at a height of 2 m (kPa), respectively, Ta is the air temperature at a height of 2 m (°C), u2 is the wind speed at a height of 2 m (m/s), Δ is the slope of the vapor pressure curve (kPa/°C), and γ is the psychometric constant (kPa/°C). Data of 2 m temperature, 2 m dew point temperature, 10 m wind speed, and surface net solar radiation were obtained from ERA-20C. The other physical quantities used in the formula were derived from these quantities in accordance with the calculation procedure of the FAO.

2.2 Data analysis

The applicability of the ERA-20C's BLH data was analysed by the corresponding period radiosonde observations data of two situs (Zhangye: 38.93°N, 100.43°E; Yuzhong: 35.87°N, 104.00°E) located on East Asia drylands during 2006-2010, which using the method of Liu et al (2010). to calculate BLH (Fig. S1). As radiosonde data started at 07:15 and 19:15 (UTC+8) and ERA-20C data were 08:00 and 20:00 (UTC+8), there was a certain difference between them in numerical value. However, the variation trend and characteristics of them are substantially in agreement, indicating that ERA-20C's BLH data are credible. Zhao et al. (2017) gained the same conclusion.

At the same time, the applicability of ERA-20C's precipitation and temperature data also analyzed by using corresponding period and higher reliability CRU data, as shown Fig. S2 and Fig. S3. The results document that the temporal variation and spatial distribution of ERA-20C are essentially in agreement with CRU.

2.3 Aridity index (AI) on dry-humid for East Asia Drylands

The AI represents the degree of climatic dryness–wetness; it is widely used in dry and wet climate

research (Huang et al., 2017). In this study, arid and semiarid regions were identified as regions with an AI of < 0.65, and they were further classified into hyper-arid (AI < 0.05), arid (0.05 ≤ AI < 0.2), semiarid (0.2 ≤ AI < 0.5), and dry sub-humid (0.5 ≤ AI < 0.65) subtypes (Middleton and Thomas 1997). The research area covered 35–50°N, 80–130°E. As there are few dry sub-humid regions in East Asia, such regions were classified as semiarid regions, and semiarid regions in this study were thus defined as regions with 0.2 ≤ AI < 0.65. The distributions of region subtypes are shown in Fig 1.

3、Results

3.1 BLH over arid and semiarid regions in East Asia

Figure 1(a) shows the spatial distribution of East Asia drylands and their subtype regions. The displayed distributions of hyper-arid, arid, and semiarid regions are similar to those found by Huang et al. (2017). Hyper-arid regions are primarily distributed in the western desert belt, which extends from the Taklamakan Desert eastward to the Badain Jaran Desert, and arid and semiarid regions are located successively surrounding hyper-arid regions. Figure 1(b) shows the spatial distribution of the BLH in East Asia drylands, where the BLH is located between 600 and 850 m. A comparison between Figures 1(a) and (b) shows that there is a close relationship between the spatial distribution of the AI and the BLH. High BLHs of more than 900 m are mainly located in hyper-arid regions, and BLHs in arid and semiarid regions decrease successively. These results demonstrate that regions with high (low) BLHs generally coincide with regions that have small (large) AI values and a relatively dry (wet) climate.

3.2 Changes in the BLH on dry-humid climate

Figure 2 shows temporal variations in the BLH and AI over the hyper-arid, arid, and semiarid regions. It is visually apparent that the BLH underwent an increasing trend (blue line) in the three subtype regions during 1900–2010, and the rates of increase in hyper-arid, arid, and semiarid regions were 1.486、4.660 和 10.413 m/10-yr, respectively, with 99% significance. The results illustrate that over the past 111 years, the ABL of the three subtype regions underwent different levels of uplift, but the most pronounced

increase occurred in semiarid regions. The AI in arid and semiarid regions exhibited a decreasing trend during 1900–2010 with rates of-2.009 $\times 10^{-3}$ and 2.025 $\times 10^{-2}$ /10-yr, respectively, with 99% significance. However, the AI in the hyper-arid region showed a slight increasing trend, but this was not found to be statistically significant. These results indicate that the arid and semiarid regions underwent drying during 1900–2010, and this effect was particularly apparent in semiarid regions.

Considering the expansion of East Asia drylands during the time period studied, the statistical scope was extended to include 30–55°N, 80–135°E when evaluating the area. Temporal variations in the BLH and the area of the EAST ASIA DRYLANDS are presented in Figure3. The BLH and the area both exhibited increasing trends, with increasing rates of 6.284 m/10-yr and 8.000×10^4 km^2/10-yr, respectively, with 99% significance. It can also be seen that the BLH and the area have a positive correlation with annual variability (with a correlation coefficient of 0.65, thus passing the 99% significance test).

3.3 Quantification of changes in the BLH on dry-humid climate

To further qualify the impacts of changes in the BLH on the degree of climatic dryness–wetness, the relationship between changes in the BLH and AI was analyzed, and the results are presented in Figure 4 , Table S1. In the hyper-arid, arid, and semiarid regions, the amplitudes of annual average BLHs were in ranges from -50 to +50, -80 to +50, and -80 to +50 m, respectively, while the amplitudes of annual AI were in ranges from -0.02 to +0.02, -0.1 to +0.1 and -0.2 to 0.2, respectively. The amplitudes of annual average BLH were almost the same in all types of areas, while the amplitudes of annual AI were the greatest in semiarid regions, followed by those in arid regions and hyper-arid regions. In addition, linear fitting was performed for changes in the height of the BLH (m) (△BLH) and changes in the quantity of the AI (△AI) for the three subtype regions, and the fitting equations are as follows,

$$\triangle AI=-2.114*10^{-4}*\triangle BLH+1.1527*10^{-4}, \quad (2)$$

$$\triangle AI=-8.861*10^{-4}*\triangle BLH+1.0123*10^{-4}, \quad (3)$$

$$\triangle AI=-1.945*10^{-3}*\triangle BLH-2.9051*10^{-4} \quad (4)$$

where △BLH is the change in the height of the BLH (m), and △AI is the change in the quantity of the AI. Figure 3(a–c) shows that in the three subtype regions, the scatters are distributed densely and evenly

on both sides of the fitting line, which indicates that there is a good linear relationship between △BLH and △AI. According to equations (2–4), in the hyper-arid, arid, and semiarid regions, with an annual average increase (decrease) of the BLH by 1 m, there is a corresponding decrease (increase) in the AI by -2.114×10^{-4}, -8.861×10^{-4} and -1.945×10^{-3}, respectively.

The impact of changes in the BLH on the range of East Asia drylands was quantitatively analyzed (Figure 3, Table S1.). For the entire East Asia drylands, the amplitude of the annual average BLH was found to be in the range of -50 to +50 m, while the amplitude of the annual area was in the range of -2×10^6 to $+2\times10^6$ km^2. The linear fitting equation for calculating △BLH with changes in the area (△area) is as follows,

$$\triangle Area=1.6*10^4*\triangle BLH-6.4*10^3 \quad (5)$$

where △BLH is the change in the BLH (m), and △Area is the change in area. As shown in Figure 5, the scatters are distributed densely and evenly on both sides of the fitting line, which indicates that there is a good linear relationship between △BLH and △Area. According to equation (5), when the annual average BLH increases (decreases) by 1 m, the area of East Asia drylands correspondingly increases (decreases) by 1.6×10^4 km^2.

3.4 Effect of changes in the BLH on dry-humid climate

A comparison between the changes in the BLH and the AI in the three subtype regions shows an evident negative correlation between both of them, and the correlation coefficients of the BLH and AI in the three subtype regions were -0.469、-0.880、-0.947, respectively.

To clarify the relationship between changes in the BLH and AI, their peak–valley values associated with annual variability were analyzed, and the results are shown in Figure 2, Table 1. In the hyper-arid regions, the peak–valley values of the BLH and AI corresponded for 68 years (accounting for 61.3%) during 1900–2010; of these, the peak (valley) values of the BLH occurred in parallel with peaks (valleys) AI values in 46 of the years (accounting for 41.4%), the BLH's peak (valley) values lagged behind the AI's valley (peak) values in 8 years (accounting for 7.2%), and the BLH's peak (valley) values were ahead of the AI's valley (peak) values in 14 years (12.6%). These results demonstrate that with respect

to the negative correlation between the BLH and AI over hyper-arid regions, approximately 20% of the corresponding peak–valley values of BLHs and AIs had an advanced or lagging relationship, and the proportion of BLH's peak (valley) values that was ahead of the AI's valley (peak) values was almost double that of BLH's peak (valley) values that lagged behind the AI's valley (peak) values.

Similar statistics were also obtained for the other two subtype regions. The results showed that there were 62 and 62 years (55.9%) in which the BLH and AI peak–valley values corresponded in the arid and semiarid regions, respectively. For arid regions, approximately 12.6% of the corresponding peak–valley values of BLHs and AIs had advanced or lagging relationships, and the proportion of the BLH's peak (valley) values that were ahead of the AI's valley (peak) values (8.1%) were almost double that of the BLH's peak (valley) values that lagged behind the AI's valley (peak) values (4.5%). For semiarid regions, approximately 15.3% of the BLHs and AI's corresponding peak–valley values had an advanced or lagging relationship, and the proportion of the BLH's peak (valley) values that was ahead of the AI's valley (peak) values (9.9%) was more than double that of the BLH's peak (valley) values that lagged behind the AI's valley (peak) values (5.4%). According to the results for the three subtype regions, it can be concluded that changes in the BLH affected the degree of climatic dryness–wetness change.

To clarify the relationship between changes in the BLH and area, a statistical analysis of their peak–valley values associated with annual variability was conducted, and the results are presented in Figure 2, Table 2. During 1900–2010, there were 59 years (53.2%) in which the BLH and area had corresponding peak–valley values. Of these, the BLH's peak (valley) values occurred in parallel with the area's peak (valley) values in 35 years (accounting for 31.5%), the BLH's peak (valley) values lagged behind the peak (valley) values of the area in 3 years (accounting for 5.4%), and the BLH's peak (valley) values were ahead of the area's peak (valley) values in 17 years (accounting for 16.2%). These results illustrate that in the positive correlation between the BLH and area of East Asia drylands, approximately 21.6% of the corresponding peak–valley values of the BLHs and the area had an advanced or lagging relationship, and the proportion of the BLH's peak (valley) values that was ahead of the area's peak (valley) values was approximately six times that of the BLH's peak (valley) values that lagged behind the area's peak (valley) values.

4、Discussion

Our analysis indicated it is consistent with current research facts and scholars' cognition, which is about associated variation trend between changes in BLH and AI as well relationships between changes in BLH and dry-wet climate changes on East Asia drylands.

ABL contributed to maintain a certain amount of moisture change on East Asia drylands, even facing with lower soil water content and also less horizontal transport of water vapor.

when the BLH increases, the ABL's atmospheric environment capacity becomes stronger relative to the original atmosphere, and then the ABL's air vapor column concentration will be decrease. In this case, it can reduce the precipitation probability, while developing atmospheric water vapor demand related to ABL. And hence surface evapotranspiration increases and latent heat (LH) flux enhances, which make terrestrial radiation assigned to sensible heat (SH) transport less, thus decreasing SH and further reducing BLH.

But, when the BLH decreases, the ABL's atmospheric environment capacity becomes weaker relative to the original atmosphere, and then the ABL's air vapor column concentration will be increase. In this case, it can strengthen the precipitation probability, while depressing atmospheric water vapor demand related to ABL. And hence surface evapotranspiration decreases and LH flux abates, which make terrestrial radiation assigned to SH transport more, thus adding SH and further increasing BLH. All the above can form a circular feedback mechanism on East Asia drylands.

In this mutual feedback, whether changes in air vapor column concentration will affect surface evapotranspiration, depends on the degree of earth surface's dryness and wetness, that is, if there is water supply on earth surface. When earth surface is very dry without water supply, surface evapotranspiration will be close to zero, thus air vapor column concentration can't cause changes in surface evapotranspiration. In this way, the above mechanism can't be fully carried out with an incomplete part that increasing (decreasing) BLH will intensify (moderate) the drying on East Asia drylands. In contrast, when earth surface has water supply, air vapor column concentration can cause changes in surface evapotranspiration, and then proceeding the complete circular feedback mechanism (in Table S1, Figure S4、S5、S6).

The quantitative analysis results in this study quantified the degree of relationship between BLH

change and climate dry-wet change, and further explained existence of the fact that changes in BLH drive climate dry-wet change, which supported the operation of the circular feedback mechanism

5、Conclusions

The temporal and spatial variation characteristics of BLH and AI and their relationship on East Asia drylands were analyzed. It is showed that high (low) BLHs generally coincide with regions that have small (large) AI values and a relatively dry (wet) climate. And during 1900–2010 the rates of increasing trend for BLH in hyper-arid, arid, and semiarid regions were 1.486、4.660 和 10.413 m/10-yr, respectively; meanwhile the rates of decreasing trend for AI in arid, and semiarid regions were -2.009×10^{-3} and 2.025×10^{-2} /10-yr; as well the BLH and the area of East Asia drylands have a positive correlation with a correlation coefficient of 0.651. Most of all, when the annual average BLH increased (decreased) by 1 m, the AI for the hyper-arid, arid, and semiarid regions correspondingly decreased (increased) by -2.114×10^{-4}, -8.861×10^{-4} and -1.945×10^{-3}, respectively, and the size of the area of East Asia drylands correspondingly increased (decreased) by 1.6×10^{4} km^2.

The BLH and AI on East Asia drylands were found to have a negative correlation with annual variability, and correlation coefficients were -0.469、-0.880 and -0.947, respectively. With respect to correspondences between the peak–valley values of BLH and AI for annual variations, 61.3%、55.9% and 55.9% of the studied years showed corresponded for hyper-arid, arid, and semiarid regions; certainly, 12.6%、8.1%、9.9% of the studied years showed changes in BLH advanced AI changes for hyper-arid, arid, and semiarid regions, respectively, which were more than the lagging relationships. Likewise, the percentage of years in which changes in BLH that were ahead of the area of East Asia drylands change was 16.2%. All of the conclusion discussed in the study indicate that there is a connection between BLH changes and climate dry-wet changes. Worthy of note, it is confirmed the phenomenon that changes in BLH drive the climate dry-wet changes on East Asia drylands.

Acknowledgments

ERA-20C data sets for this paper are available at the European Centre for Medium-Range Weather Forecast (http://apps.ecmwf.int /datasets/). This work was jointly

supported by the National Natural Science Foundation of China under grant (41875085、41630421、41741023).

References

Ahlgrimm M and Randall D A (2006) Diagnosing monthly mean boundary layer properties from reanalysis data using a bulk boundary layer model. Journal of the Atmospheric Sciences. 63: 998-1012.

Brewer M J, Heim R R (2011) International drought workshop series. Bull Amer Meteor Soc. 92: 29-31.

Compton J C, Delgado R, Berkoff T A, Hoff R M (2013) Determination of Planetary Boundary Layer Height on Short Spatial and Temporal Scales: A Demonstration of the Covariance Wavelet Transform in Ground-Based Wind Profiler and Lidar Measurement. Journal of Atmospheric and Oceanic Technology. 30: 1566-1575.

Dai A (2013) Increasing drought under global warming in observations and models. Nature Climate Change. 3: 52-58.

Davy, R. and Esau, I (2016) Differences in the efficacy of climate forcings explained by variations in atmospheric boundary layer depth. Nat. Commun. 7: 11690.

Esau I N (2008) Formulation of the planetary boundary layer feedback in the Earth's climate system. Institute of Computational Technologies Sb Ras Novosibirsk. 13: 90-103.

Esau I, Zilitinkevich S (2010) On the role of the planetary boundary layer depth in the climate system. Advances in Science and Research. 4: 63-69. https://doi.org/10.5194/asr-4-63-2010.

ECMWF. IFS Documentation CY40R1. Operational implementation 22 November (2013) PART IV: PHYSICAL PROCESSES [R].2014, pp50.

Huang J., Li Y., Fu C., Chen F., Fu Q., Dai A., Shinoda M., Ma Z., Guo W., Li Z., Zhang L., Liu Y., Yu H., He Y., Xie Y., Guan X., Ji M., Lin L., Wang S., Yan H., Wang G. (2017) Dryland climate change: Recent progress and challenges. Rev. Geophys. 55: 719–778. https://doi.org/10.1002/2016RG000550.

Itano T (1998) Synoptic disturbance and rainfall over the arid area in the Northwest China. Journal of the Meteoro logical Society of Japan. 76: 325-333.

Ji, M., Huang J, Xie Y., Liu J. (2015) Comparison of dryland climate change in observations and CMIP5 simulations. Adv. Atmos. Sci. 32: 1565–1574. https://doi.org/10.1007/s00376-015-4267-8.

Li Y., Qian Z., Xue X., Lan X., Li L. (2009) Deep Mixed Layer in Northwest China Dry Area in Summer Half Year and Formation of the Dry Climate. Chinese Plateau Meteorology, 28 (1): 46−54, doi: http://ir.casnw.net/handle/362004/20238.

Liu S Y, Liang X Z (2010) Observed diurnal cycle climatology of planetary boundary layer height. Journal of Climate. 23: 5790－5809.

Li Y., Zhang Q., Hu X., Wang R. (2012) Atmosphere boundary layer characteristics and their responses to wetness change over arid regions and loess plateau in northwest China. Chinese Journal of Glaciology and Geocryology. 34(5): 1048-1058.

Marsham J H, Parker D J, Crams C M, Grey W M F, Johnson B T (2008) Obsevations of mseoscale and boundary-layer circulation affecting dust uplift and transport in the Saharan boundary-layer. Atmo Chem Phys Discuss. 8: 8817-8845.

McGrath-Spangler E L (2016) The impact of a boundary layer height formulation on the GEOS-5 model climate. J. Geophys. Res.-Atmos. 121: 3263-3275. https://doi.org/10.1002/2015JD024607.

Poli, P., H. Hersbach, D. P. Dee, P. Berrisford, A. J. Simmons, F. Vitart, P. Laloyaux, D. G. H. Tan, C. Peubey, J.-N. Thépaut, Y. Trémolet, E. V. Hólm, M. Bonavita,L. Isaksen, and M. Fisher. (2016) ERA-20C: An atmospheric reanalysis of the twentieth century. J. Climate. 29, 4083–4097. https://doi.org/10.1175/JCLI-D-15-0556.1.

Rosenfeld D, Mintz Y (1988) Evaporation of rain falling from convective clouds as derived from radar measurement. Journal of Applied Meteorology & Climatology. 27: 209-215.

Reddy K K, Toshiaki K, Yuichi O (2002) Planetary boundary layer and precipitation studies using lower atmospheric wind profiler over tropical India. Radio Science. 37: 1-21.

Schmid P, Niyogi D (2021) A method for estimating planetary boundary layer heights and its application over the ARM Southern Great Plains Site. Journal of Atmospheric and Oceanic Technology. 29(3): 316-322.

Takemi T (1999) Structure and evolution of a severe squall line over the arid region in northwest China. Mon Weather Rev. 127: 1301–1309.

Trenberth K E, Dai A, van der Schrier G, Jones Philip D, Barichivich Jonathan, Briffa Keith R, Sheffield Justin (2014) Global warming and changes in drought. Nature Climate Change. 4: 17-22.

You H., Liu W., Tan J. (2010) Temporal characteristics of atmospheric maximum mixing depth of Beijing. Chinese Meteorological Monthly. 36: 51−55. doi: 10.3788/HPLPB20102207.1462.

White, R. P., and J. Nackoney (2003), Dryland s, People and Ecosystem Goods and Services, World Resources Institute, Washington.

Wang J., Cai X., Song Y. (2016) Daily maximum height of atmospheric boundary layer in Beijing: Climatology and environmental meaning. Chinese Climatic and Environmental Research. 21 (5): 525−532. doi:10.3878/j.issn.1006-9585.2016.15178.

Zhang L, Zhou T (2015) Drought over East Asia: a review. Journal of Climate. 28(8): 3375-3399.

Zhao Y., Mao W., Zhang K., Ma Y., Li H., Zhang W. (2017) Climatic Variations in the Boundary Layer Height of Arid and Semiarid Areas in East Asia and North Africa. Journal of the Meteorological Society of Japan. 95: 181-197. https://doi.org/10.2151/jmsj.2017-010.

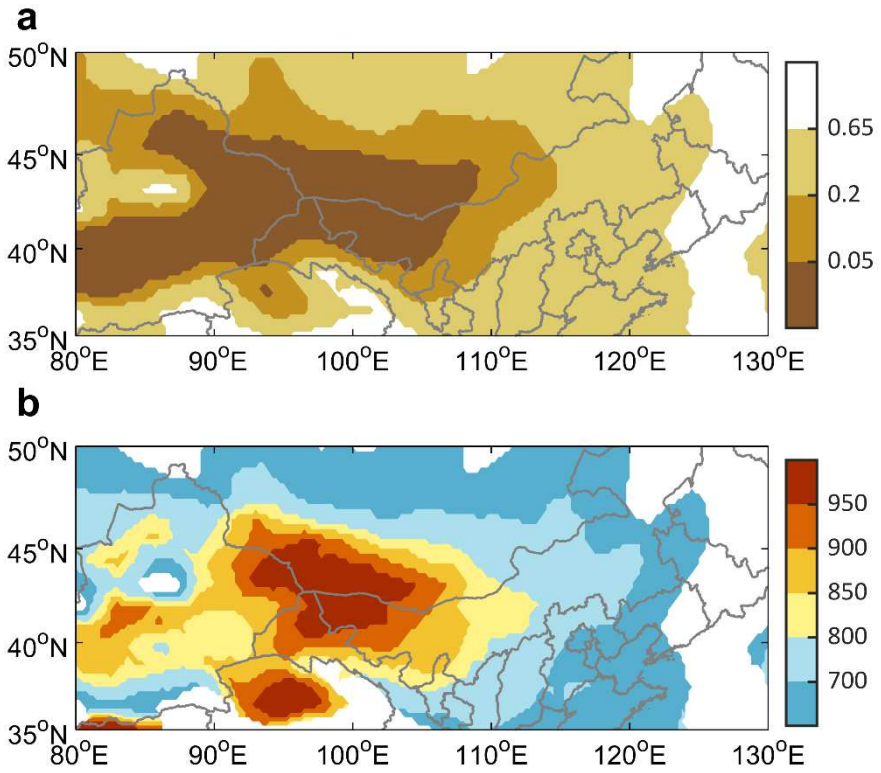

Figure 1: Distributions of climatological (1900–2010) annual mean (a) AI and (b) BLH over arid and semiarid regions in East Asia.

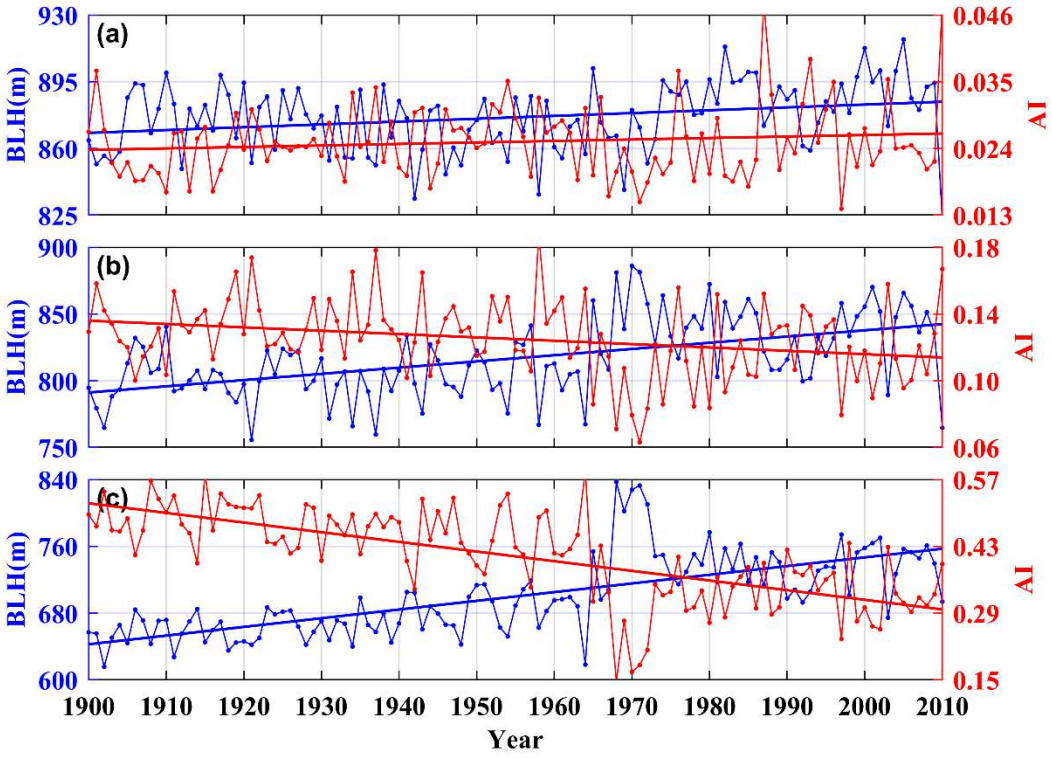

Figure 2: Mean time series of BLH (blue) and AI (red) during 1900-2000 in (a) hyper-arid, (b) arid, and (c) semiarid regions.

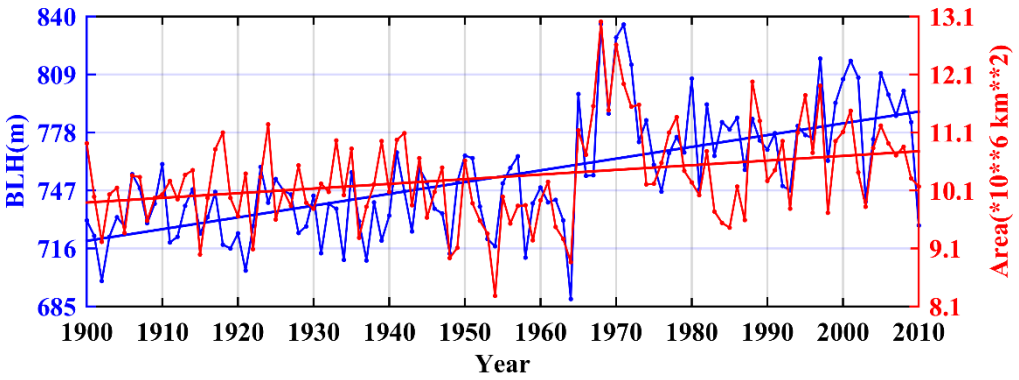

436

437 **Figure 3: Mean time series of BLH (blue) and Area (red) of East Asia drylands during 1900-2000.**

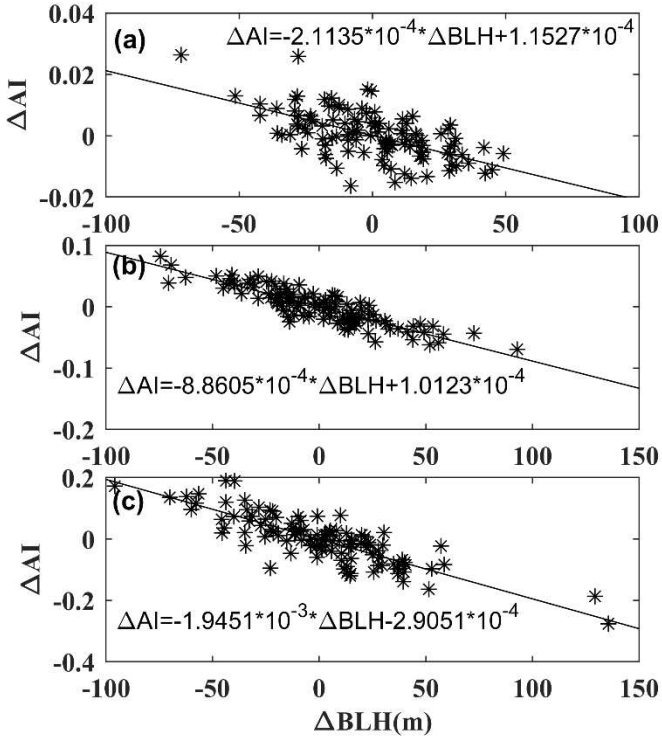

438

439 **Figure 4: Scatter plot of changes in the BLH and AI in (a) hyper-arid, (b) arid, and (c) semiarid regions.**

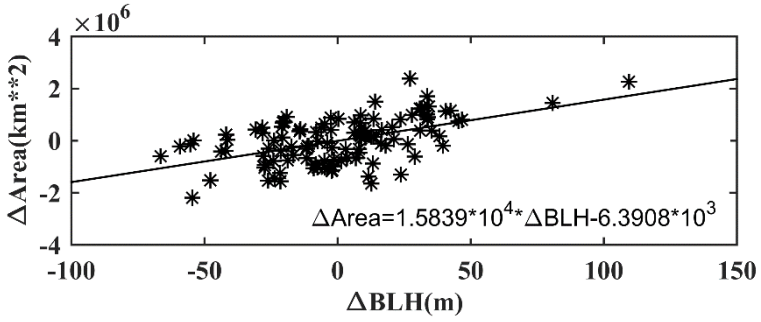

440

441 **Figure 5: Scatter plot of changes in the BLH and Area in East Asia drylands.**

442

443 **Table 1: BLH and AI peaks and valleys over subtype regions (P = peak; V = valley).**

Regions	The BLH's peak (valley) values occur in parallel with the AI's valley (peak) values	The BLH's peak (valley) values lag behind the AI's valley (peak) values	The BLH's peak (valley) values ahead of the AI's valley (peak) values
Hyper-arid regions	1901V/P, 1906P/V, 1908V/P,1910P/V, 1912V/P, 1913P/V, 1919V/P, 1920P/V, 1921V/P, 1923P/V, 1924V/P, 1929V/P, 1930P/V, 1931V/P, 1934V/P, 1935P/V, 1937V/P, 1938P/V, 1939V/P, 1946V/P, 1947P/V, 1948V/P, 1952V/P, 1953P/V, 1954V/P, 1957P/V, 1958V/P, 1959P/V, 1961V/P, 1963P/V, 1964V/P, 1965P/V, 1969V/P, 1974P/V, 1976V/P, 1980P/V, 1981V/P, 1987V/P, 1989P/V, 1990V/P, 1991P/V, 1993V/P, 1996V/P, 1997P/V, 1998V/P, 2003V/P	1917P/1916V, 1927P/1926V, 1945P/1944V, 1951P/1950V, 1968P/1967V, 1995P/1994V, 2002P/2001V, 2005P/2004V,	1905P/1906V, 1914V/1915P, 1915P/1916V, 1925P/1926V, 1926V/1927P, 1927P/1928V, 1933V/1934P, 1940P/1941V, 1942V/1943P, 1970P/1971V, 1978V/1979P, 1982P/1983V, 1983V/1984P, 2000P/2001V
Arid regions	1906P/V, 1910P/V, 1911V/P, 1915V/P, 1916P/V, 1919V/P, 1920P/V, 1921V/P, 1923P/V, 1927P/V, 1930P/V, 1931V/P, 1933P/V, 1934V/P, 1935P/V, 1937V/P, 1941P/V, 1943V/P, 1944P/V, 1950P/V, 1952V/P, 1953P/V, 1954V/P, 1957P/V, 1958V/P, 1961V/P, 1964V/P, 1965P/V, 1968P/V, 1969V/P, 1973V/P, 1974P/V, 1976V/P, 1978P/V, 1979V/P, 1980P/V, 1981V/P, 1982P/V, 1991P/V, 1992V/P, 1994P/V, 1997P/V, 1998V/P, 2001P/V, 2003V/P, 2005P/V, 2007V/P, 2008P/V	1902V/1901P, 1914P/1913V, 1948V/1947P, 1963P/1962V, 1967V/1966P	1908V/1909P, 1924V/1925P, 1928V/1929P, 1948V/1949P, 1970P/1971V, 1983V/1984P, 1985P/1986V, 1989V/1990P 1995V/1996P,
Semiarid regions	1902V/P, 1904P/V, 1905V/P, 1906P/V, 1908V/P, 1910P/V, 1911V/P, 1914P/V, 1915V/P, 1923P/V, 1926P/V, 1928V/P, 1930P/V, 1931V/P, 1934V/P, 1935P/V, 1937V/P, 1938P/V, 1939V/P, 1943V/P, 1944P/V, 1951P/V, 1954V/P, 1957P/V, 1964V/P, 1965P/V, 1966V/P, 1968P/V, 1969V/P, 1976V/P, 1979V/P, 1980P/V, 1981V/P, 1982P/V, 1985V/P, 1986P/V, 1987V/P, 1988P/V, 1990V/P, 1997P/V, 1998V/P, 2002P/V, 2003V/P, 2007V/P, 2008P/V	1917P/1916V, 1918V/1917P, 1948V/1947P, 1962P/1961V, 1971P/1970V, 1978P/1977V	1920P/1921V, 1921V/1922P, 1923P/1924V, 1924V/1925P, 1932P/1933V, 1941P/1942V, 1958V/1959P, 1991P/1992V, 1992V/1993P, 1999P/2000P, 2005P/2006V

444

445 **Table 2: BLH and Area peaks and valleys (P = peak; V = valley).**

	The BLH's peak (valley) values occur in parallel with the area's peak (valley) values	The BLH's peak (valley) values lag behind the area's peak (valley) values	The BLH's peak (valley) values ahead of the area's peak (valley) values
Years	1902V, 1904P, 1905V, 1906P, 1908V, 1914P, 1915V, 1934V, 1935P, 1943V, 1944P, 1948V, 1954V, 1964V, 1965P, 1966V, 1968P, 1969V, 1979P, 1981V, 1982P, 1985V, 1986P, 1987V, 1988P, 1990V, 1993V, 1996V, 1997P, 1998V, 2001P, 2003V, 2005P, 2007V, 2008P	1921/1920V, 1928/1927V, 1931/1930V, 1932/1931P, 1937/1936V, 1972/1971P	1910/1911P, 1911/1912V, 1917/1918P, 1919/1920V, 1920/1921P, 1921/1922V, 1923/1924P, 1924/1925V, 1925/1926P, 1931/1932V, 1932/1933P, 1939/1940V, 1958/1959V, 1960/1961P, 1973/1974V, 1991/1992P,

446

Figures

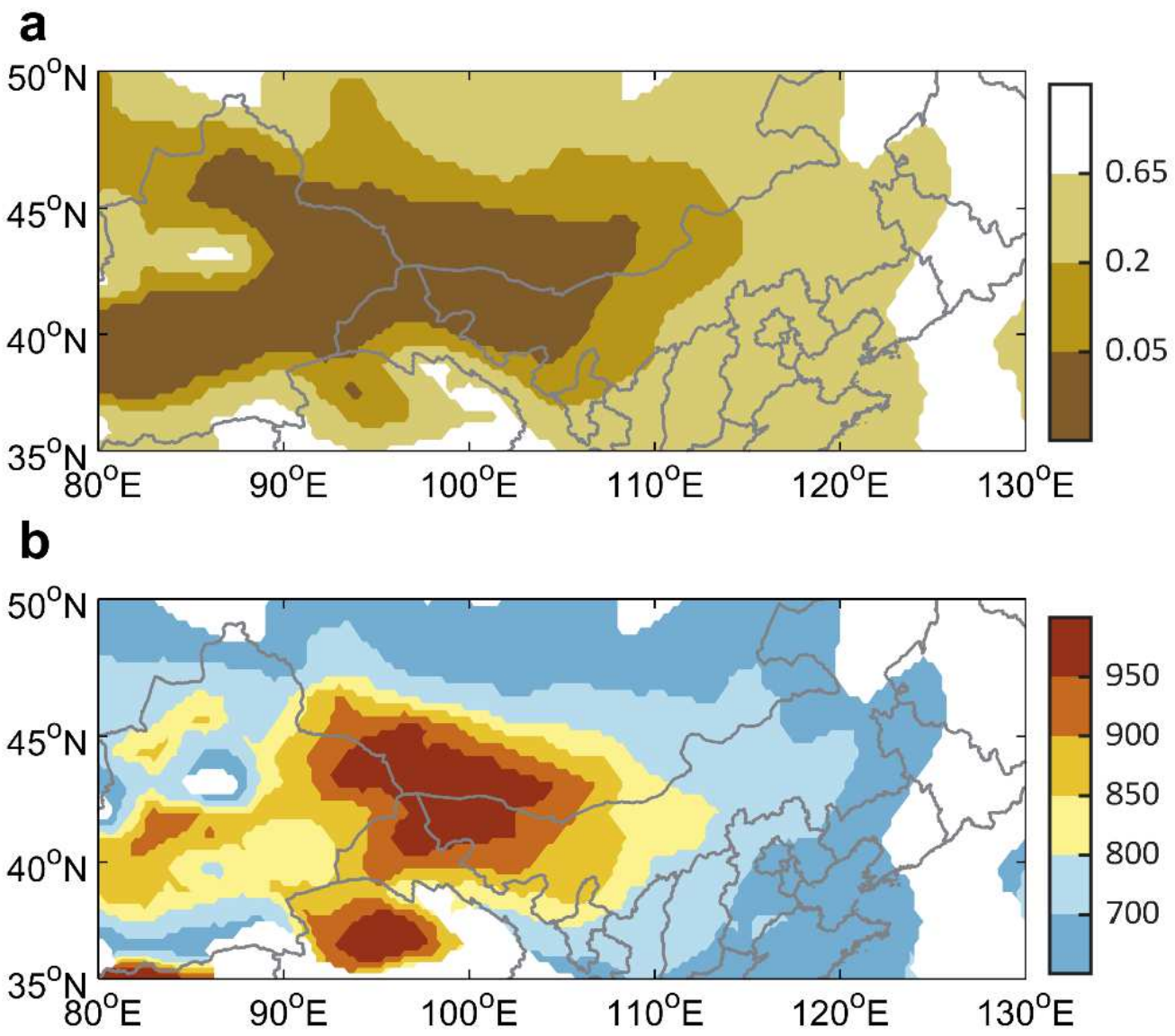

Figure 1

Distributions of climatological (1900–2010) annual mean (a) AI and (b) BLH over arid and semiarid regions in East Asia.

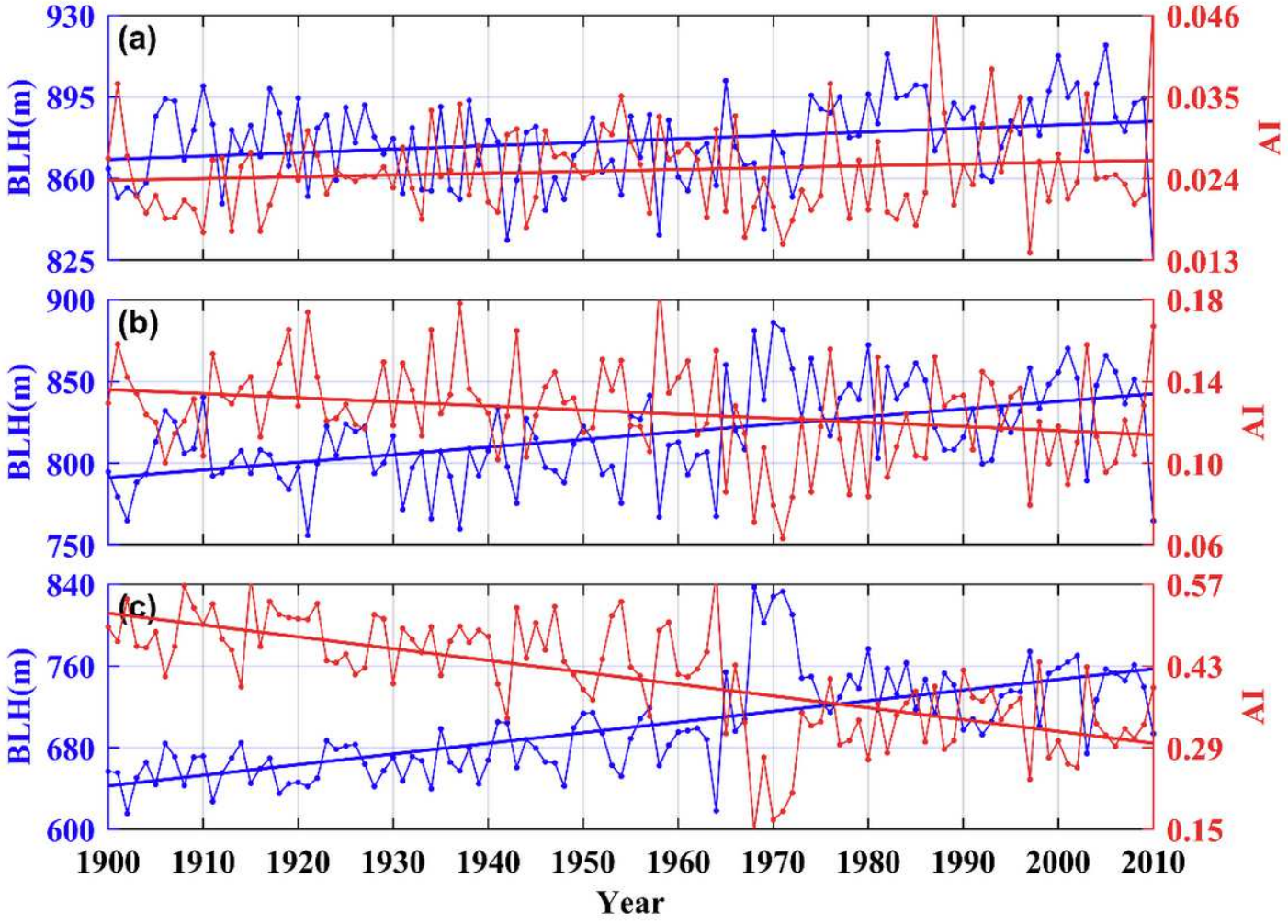

Figure 2

Mean time series of BLH (blue) and AI (red) during 1900-2000 in (a) hyper-arid, (b) arid, and (c) semiarid regions.

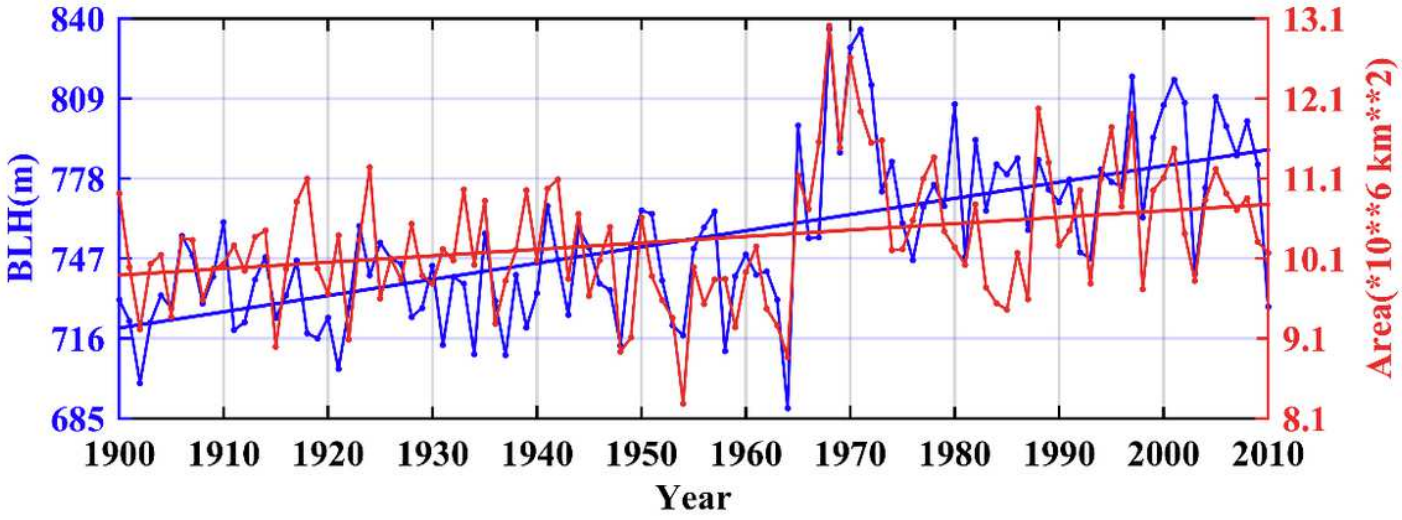

Figure 3

Mean time series of BLH (blue) and Area (red) of East Asia drylands during 1900-2000.

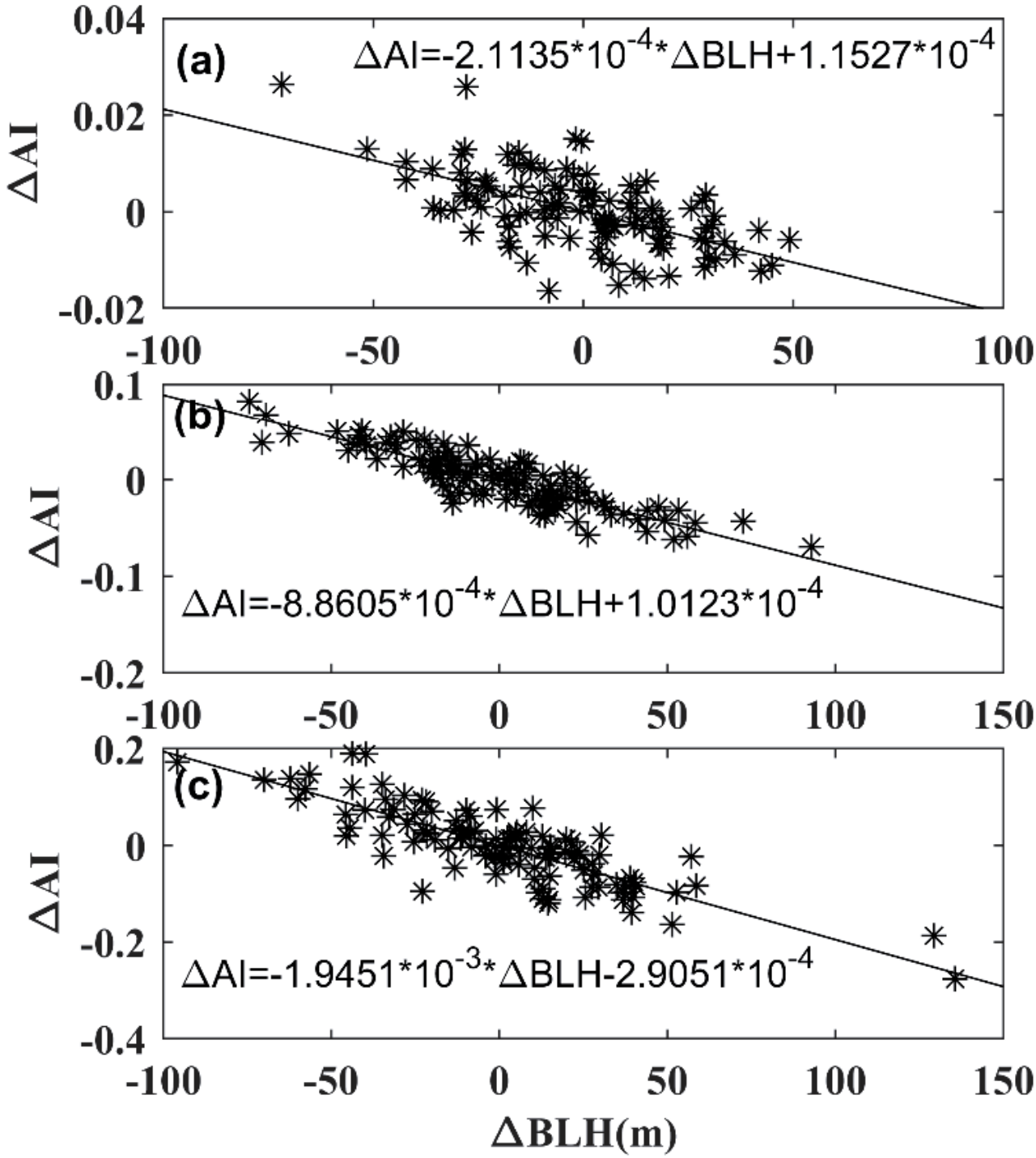

Figure 4

Scatter plot of changes in the BLH and AI in (a) hyper-arid, (b) arid, and (c) semiarid regions.

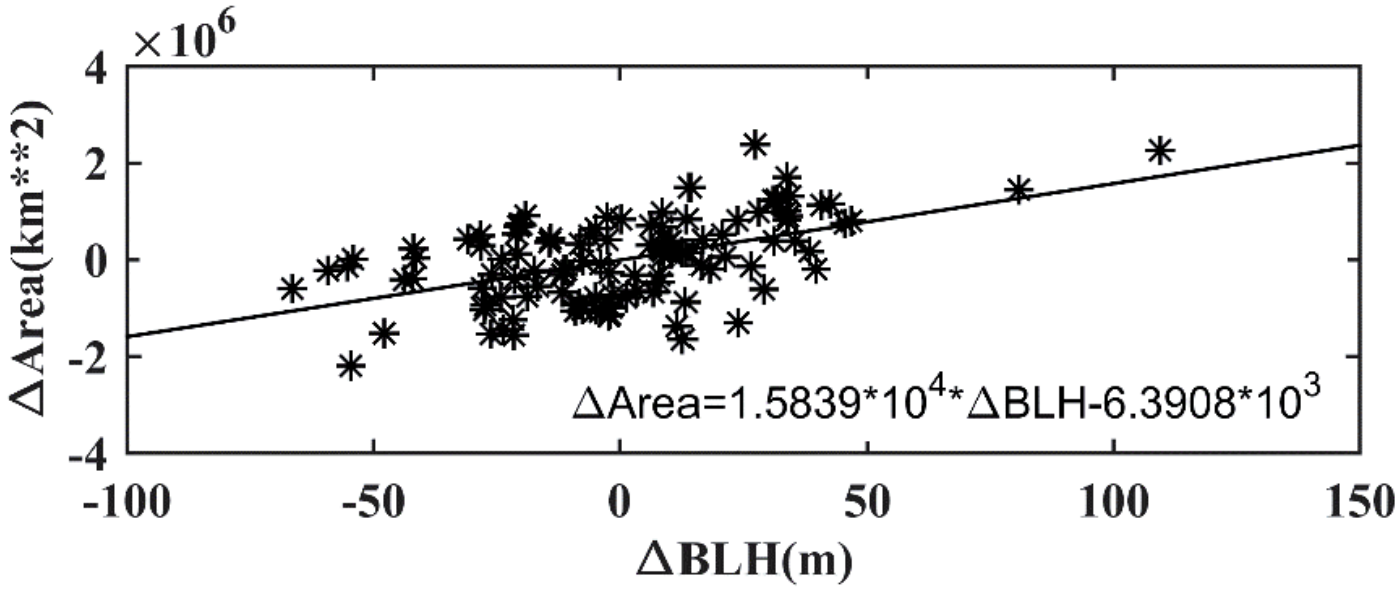

Figure 5

Scatter plot of changes in the BLH and Area in East Asia drylands.

Supplementary Files

This is a list of supplementary files associated with this preprint. Click to download.

- Additionaldocument.docx